Published in final edited form as:
Anal Chem. 2013 January 2; 85(1): 10–13. doi:10.1021/ac3029129.

High-Resolution Differential Ion Mobility Spectrometry of a Protein

Alexandre A. Shvartsburg and **Richard D. Smith**
Biological Sciences Division, Pacific Northwest National Laboratory, P.O. Box 999, Richland, WA 99352

Abstract

Use of elevated electric fields and helium-rich gases has recently enabled differential IMS with resolving power up to $R \sim 300$. Here we applied that technique to a protein (namely, ubiquitin), achieving R up to ~80 and separating many previously unresolved conformers. While still limited by conformational multiplicity, this resolution is some four times greater than that previously reported using either conventional (drift-tube or traveling-wave) or differential IMS. The capability for fine resolution of protein conformers may open new avenues for proteoform separations in top-down and intact-protein proteomics.

Introduction

Ion mobility spectrometry (IMS), the approach to separation and characterization of ions exploiting their transport through gases driven by electric field, consists of two branches:[1,2] conventional IMS based on the absolute ion mobility (K) and differential or field asymmetric waveform IMS (FAIMS) relying on the difference (Δ) between K values at high and low electric field intensity (E). Both methods, combined with mass spectrometry (MS), have been utilized to investigate proteins and other biomolecules since 1990-s.[3,4] With conventional drift-tube (DT) IMS, the K quantity can be related to ion geometries by *a priori* calculations, which has revealed much about the protein folding and quaternary structure of protein complexes.[3,5–9] That approach is still constrained by modest observed resolving powers ($R < \sim 20$) that reflect the multiplicity of geometries within each separated structural family (e.g., folded or unfolded) rather than instrumental limitations.[5,7] Hence DT IMS resolution of proteins has barely improved since early days, despite major gains of instrumental R (to >200 for multiply-charged peptides).[10] In a powerful capability for fundamental explorations, two-dimensional IMS platforms[11,12] enable slicing broadened peaks at the end of Stage 1 to pass specific subpopulations with the width governed by instrumental R, then probing the selected conformers in Stage 2. Still, dramatic broadening of original features due to conformational variability obstructs IMS separations of primary structure isomers such as sequence inversions or localization variants with post-translational modifications (PTMs) on alternative sites. Such species have been broadly resolved for peptides (that have instrumentally-controlled peak widths) at $R \sim 100$,[13,14] and their separation for whole proteins would greatly benefit top-down proteomics.

The use of FAIMS to elucidate macromolecular structures has been impeded by two problems: (i) the ΔK quantity could not be computed from ion geometries so far,[2] and (ii) heating of ions above the gas temperature T by strong fields in FAIMS routinely distorts fragile structures, including tertiary protein folds.[2,15,16] The conundrum here is that the field heating magnitude ΔT scales as E^2:

$$\Delta T = M(KE)^2/3k \quad (1)$$

(where M is the gas molecule mass and k is the Boltzmann constant).[15,16] As MK^2 is proportional to $1/\Omega^2$ (where Ω is the ion-molecule collision cross section), ΔT by eq (1) increases upon addition of lighter gases[17–19] such as He or H_2 which have lower Ω values than N_2 with any ion.[17] Thus, as the resolving power generally scales as E^3 and is improved in light gas mixtures,[2,18–20] the conditions benefiting the separation inherently augment structural distortions. However, (i) FAIMS is much more orthogonal to MS than conventional IMS is[21] and therefore tends to distinguish isomers better at equal formal R values and (ii) use of stronger electric fields and buffers rich in He or H_2 has raised[19,20,22] FAIMS resolving power for multiply-charged peptides up to ~300, matching and exceeding the metrics for conventional IMS/MS systems.[10] These factors allow FAIMS to broadly separate sequence and PTM localization isomers for peptides.[19,22–24] Previous FAIMS studies of proteins have also not achieved $R > 20$, but the analyzers involved had instrumental R of just ~10 – 30 and thus what capped the attained resolution remained undetermined.[7,15,16,25–29]

Here, we report first analyses of proteins using high-resolution FAIMS. With bovine ubiquitin (Ub, 8565 Da) - the prototypical model protein in MS and IMS, the resolving power reaches ~80 for higher charge states and many more features than in the previous FAIMS data are resolved. We anticipate this performance to engender new FAIMS applications to (at least smaller) intact proteins.

Experimental

In FAIMS, ions are pulled by gas flow through a gap between two electrodes while filtered in a periodic asymmetric field $E(t)$ of some amplitude (E_D) created by a waveform loaded on those electrodes.[2] The net drift of any given species across the gap can be offset by a fixed "compensation field" (E_C) added to $E(t)$. Thus equilibrated ions can exit the unit and be detected, and scanning E_C yields a spectrum.[2] The FAIMS resolving power strongly depends on the gap geometry: planar designs with homogeneous field can provide much higher resolution than the curved devices.[29]

We used a planar FAIMS unit coupled to a Thermo LTQ ion trap[18–20,22,24] with about the highest implemented E_D = 28 kV/cm. The He/N_2 gas mixtures with up to 50% He (the maximum avoiding electrical breakdown)[18] were supplied at 2 L/min, leading to the standard ion residence time of 0.2 s. Ions were derived from electrospray ionization (ESI) of ~10 μM solution of Ub in 50:49:1 water/methanol/acetic acid, infused to the emitter at ~0.5 μL/min.

Results and discussion

As usual with a denaturing solvent,[6,15,16] ESI has generated protonated Ub ions with z = 5 – 13. The FAIMS spectra as a function of He content and benchmarks obtained[7] employing a cylindrical unit at E_D = 20 kV/cm with N_2 are shown in Figure 1 (the spectra from cylindrical and planar units at E_D = 20 kV/cm were compared previously).[29] Raising E_D has expectedly moved all spectra to higher E_C, but changes go beyond that because of improved resolution and stronger field heating: by eq (1), the ΔT value at E_D = 28 kV/cm is nearly double that at 20 kV/cm. With N_2 gas, Ub^{5+} and Ub^{6+} still exhibit a single dominant peak: these low-charged species adopt stable compact shapes unaffected by moderate heating.[6,15,16] For z = 7 – 9, stronger Coulomb repulsion destabilizes such geometries and unwraps them via multiple partly folded intermediates, with the conformer distributions sensitive to the ion temperature ($T_I = T + \Delta T$) and experimental timescale.[6,15] In FAIMS, unfolding of peptides or proteins is normally manifested by emergence and growth of lower-E_C features.[15,16,26] Indeed, the present ratio of elongated **a** and more compact **b** conformers

for $z = 7 – 9$ is much shifted toward **a** compared to the benchmarks,[7] with **b** almost vanishing for Ub^{9+} (Figure 1). For $z = 10 – 13$, the protein was fully unfolded[7] at lower E_D and remains unfolded, but improved resolving power leads to the emergence of feature **a** on the low-E_C side for Ub^{10+} and partial separation of two peaks for Ub^{12+}. As the latter was seen (although less well) using the same planar analyzer at $E_D = 20$ kV/cm,[29] this resolution gain arises from both higher E_D and the intrinsic advantage of planar geometry.[29]

The peak widths (fwhm) for $z = 5$ and $8 – 13$ fall in the range of $w = 3.1 – 4.7$ V/cm, while the much larger $w = 5.8$ V/cm for Ub^{6+} and $w = 8.7$ V/cm for Ub^{7+} indicate congestion of unresolved geometries (Figure 2). For each z, these values are smaller than those with the cylindrical FAIMS unit[7] and overall compare to those with same planar device[29] at lower $E_D = 20$ kV/cm (Figure 2), which makes sense as w should not materially depend on E_D (with planar gaps).[30] The resolving power broadly increases over both benchmarks because of higher E_C, to $R = 10 – 25$ from $6 – 10$ for cylindrical unit[7] and $8 – 20$ for this planar device[29] at $E_D = 20$ kV/cm. However, the result is still within or close to the limits previously demonstrated for FAIMS or DT IMS. With planar FAIMS analyzers, the peak widths scale approximately as $(Kz)^{-1/2}$: the features are narrower for species of greater mobility and/or charge.[30,31] The mobilities of Ub ions with $z = 6 – 13$ in N_2 at room temperature are[15] are $K \sim 0.85 – 1.3$ $cm^2/(Vs)$, which is close to the values for 2+ peptides such as nine-residue bradykinin (1060 Da) with measured[17] $K \sim 1.3$ $cm^2/(Vs)$ and 15-residue τ-phosphopeptides (1603 Da) with $K \sim 1.0$ $cm^2/(Vs)$ estimated from the established mass/mobility trend line.[10] The features for these peptides in same FAIMS regime have[18,23] $w \sim 1.6 – 2.2$ V/cm. When adjusted for the higher charge of Ub ions, those values would translate into $w = 0.6 – 1.4$ V/cm overall and $0.6 – 1.1$ V/cm for $z = 8 – 13$. Hence the present peaks for Ub with $z \geq 8$ are broader than the instrumental limits by $3 – 7$ times.

As for peptides,[18,22–24] raising the He fraction moves all spectra to yet higher E_C while promoting unfolding (Figure 1). While Ub^{5+} exhibits no elongated structures at lower E_C up to the maximum He content, their fractional abundances increase monotonically from ~2% to ~50% for Ub^{6+} and from ~50% to ~100% for Ub^{7+} and Ub^{8+}. As predicted in theory and verified for peptides and other ions,[18–20,22–24] addition of He raises K values and thus (with planar FAIMS devices) narrows the peak for any defined species, typically by ~20 – 30% on the way from N_2 to 1:1 He/N_2 as the peptide mobilities increase by ~50 – 60%. Here, the widths decrease for $z = 8 – 13$ by a greater $1.5 – 2.8$ times (albeit not uniformly), stay flat for $z = 7$, and increase by $1.7 – 2.1$ times for $z = 5$ and 6 (Figure 2). These data mean that the number and diversity of unresolved conformers expand for Ub^{5+} and Ub^{6+} that begin unfolding in the relevant T_I range, but decrease for higher z as unfolded structures anneal to fewer delineated basins. As E_C values increase while peaks narrow, the resolving power rapidly improves and reaches ~60 for $z = 8$ and 9 and ~80 for $z = 10 – 13$ (Figure 2). These are the highest R metrics reported for proteins using FAIMS, which allows distinguishing up to 5 conformers (seen for $z = 11$ and 12). Yet, the peak widths of $1.7 – 2.2$ V/cm for $z = 8 – 13$ (at 50% He) are $2 – 3$ times greater than those for above 2+ peptides[18,23] ($w = 1.5 – 1.8$ V/cm) upon adjustment to $z = 8 – 13$. Thus even the narrowest features here still comprise multiple conformers, although to a lesser extent than those found using N_2.

Comparisons of conformer distributions observed for $z = 6 – 10$ in FAIMS and 2-D FAIMS/DTIMS with those encountered in DTIMS upon thermal heating of ions[6] permit gauging T_I values in FAIMS.[15] At $E_D = 20$ kV/cm, thus estimated T_I was[15] 68 – 76 °C. The conformer populations in present spectra at $E_D = 28$ kV/cm with N_2 (Figure 1) closely mirror those measured[6] in DTIMS at $T = 76$ °C for Ub^{6+} (with a slight onset of unfolding in **a**), but $T = 97$ °C for Ub^{7+} (with equally abundant folded and unfolded families), Ub^{8+} (with a sharp primary peak for unfolded conformers and substantial broad feature for more compact species), and Ub^{9+} (with no folded geometries). The populations in FAIMS at 50% He best

match those in DTIMS at T = 117 – 132 °C, with (partly) folded features competing with the elongated family for Ub^{6+}, dropping to a significant shoulder for Ub^{7+}, and totally vanishing for Ub^{8+}.

Further, one may apply eq (1) to calculate[15,18] time-averaged T_I over the waveform cycle ($<T_I>$) and maximum T_I at the peak (T_{max}). The T_I values matched to DTIMS data fall between thus computed $<T_I>$ and T_{max} for "compact" structures in all regimes (Table 1), supporting the argument that unfolding of those structures (and, generally, macromolecular transformations) in FAIMS is largely controlled by the maximum rather than average ion temperature over the waveform cycle.[15] That T_I at E_D = 20 kV/cm amounts to ~75 – 90 % of T_{max} has been rationalized[15] by noting that T_{max} applies only at the waveform peak, while isomerization requires time (especially for large molecules) and thus the ion temperature must be averaged over a finite segment around the maximum E. The shortfall grows at E_D = 28 kV/cm (where T_I falls to ~65 – 75% of T_{max}), which is hard to explain in the same way as identical waveform profiles should lead to similar adjustment factors regardless of the amplitude. However, the real T_I is determined by the instantaneous mobility of an isomerizing ion, not its initial geometry. Thus substituting the K values for compact shapes into eq (1) may be reasonable at lower temperatures where unfolding begins, but not for extensively denatured proteins at higher temperatures (Figure 1). As ion temperatures are proportional to K^2, unfolding (which typically increases cross sections, thus decreasing mobility) may substantially attenuate the field heating. Indeed, the T_{max} values computed for unfolded Ub geometries agree with the measurements well (Table 1).

If the drastic peak narrowing upon He addition reflects a reduced conformational diversity upon annealing induced by stronger field heating, one may ask why no such narrowing is evident in the DT IMS data obtained[6] at similar T = 117 – 132 °C. An obvious explanation is that present analyses take much longer (~200 ms) than those DT IMS separations (~10 – 20 ms),[6,32] permitting a more complete annealing. Another possibility is that conformers that substantially evolve and change E_C during FAIMS filtering (beyond the onset stage of ~10 ms) are removed by "self-cleaning", leaving more stable and better-defined conformers to be observed.[15] A similar mechanism supposedly eliminates isomerizing conformers in overtone mobility spectrometry (OMS) filtering, where high resolving powers are also achievable with longer analyses.[33]

Conclusions

In the first application of high-resolution FAIMS analyses to proteins using He/N_2 gas, we have reached a resolving power up to ~80 or roughly four times the previous maximum. This allowed resolution of heretofore "co-eluting" conformers, up to five for unfolded ubiquitin ions. We expect more conformers distinguished for larger proteins that tend to occupy a wider separation space,[7,15] especially those above ~30 kDa covering enormous E_C ranges (presumably because of dipole alignment).[28] The field heating of protein ions to the maximum temperatures of ~120 – 180 °C causes major isomerization, and, importantly, apparent annealing of unfolded geometries into fewer and/or closer deep wells on the energy surface. However, the observed peak widths are still limited by conformational multiplicity. Replacing He in He/N_2 mixtures with H_2 permits light gas fractions up to ~85%, which generally improves resolution for peptides (including larger ones).[19,22] A similar benefit for proteins is likely.

Acknowledgments

We thank Dr. Keqi Tang and Ron Moore for experimental help and Prof. David Clemmer for insightful discussions. This work was supported by NIH NIGMS (8 P41 GM103493-10) and US DoE OBER (Panomics Project), and carried out in the Environmental Molecular Sciences Laboratory, a DoE national scientific user facility at PNNL.

References

1. Eiceman, GA.; Karpas, Z. Ion Mobility Spectrometry. CRC Press; Boca Raton, FL: 2005.
2. Shvartsburg, AA. Differential Ion Mobility Spectrometry: Nonlinear Ion Transport and Fundamentals of FAIMS. CRC Press; Boca Raton, FL: 2008.
3. Hoaglund-Hyzer CS, Counterman AE, Clemmer DE. Chem Rev. 1999; 99:3037– 3079. [PubMed: 11749510]
4. Purves RW, Guevremont R. Anal Chem. 1999; 71:2346–2357. [PubMed: 21662783]
5. Hudgins RR, Woenckhaus J, Jarrold MF. Int J Mass Spectrom Ion Processes. 1997; 165/166:497–507.
6. Li J, Taraszka JA, Counterman AE, Clemmer DE. Int J Mass Spectrom. 1999; 185/186/187:37–47.
7. Shvartsburg AA, Li F, Tang K, Smith RD. Anal Chem. 2006; 78:3304–3315. ibid 8575. [PubMed: 16689531]
8. Ruotolo BT, Giles K, Campuzano I, Sandercock AM, Bateman RH, Robinson CV. Science. 2005; 310:1658–1661. [PubMed: 16293722]
9. Uetrecht C, Rose RJ, van Duijn E, Lorenzen K, Heck AJR. Chem Soc Rev. 2010; 39:1633–1655. [PubMed: 20419213]
10. Srebalus CA, Li J, Marshall WS, Clemmer DE. Anal Chem. 1999; 71:3918–3927. [PubMed: 10500479]
11. Koeniger SL, Merenbloom SI, Clemmer DE. J Phys Chem B. 2006; 110:7017–7021. [PubMed: 16571016]
12. Koeniger SL, Clemmer DE. J Am Soc Mass Spectrom. 2007; 18:322–331. [PubMed: 17084091]
13. Wu C, Siems WF, Klasmeier J, Hill HH. Anal Chem. 2000; 72:391–395. [PubMed: 10658335]
14. Ibrahim Y, Shvartsburg AA, Smith RD, Belov ME. Anal Chem. 2011; 83:5617–5623. [PubMed: 21692493]
15. Shvartsburg AA, Li F, Tang K, Smith RD. Anal Chem. 2007; 79:1523–1528. [PubMed: 17297950]
16. Robinson EW, Shvartsburg AA, Tang K, Smith RD. Anal Chem. 2008; 80:7508–7515. [PubMed: 18729473]
17. Baker ES, Clowers BH, Li F, Tang K, Tolmachev AV, Prior DC, Belov ME, Smith RD. J Am Soc Mass Spectrom. 2007; 18:1176–1187. [PubMed: 17512752]
18. Shvartsburg AA, Prior DC, Tang K, Smith RD. Anal Chem. 2010; 82:7649–7655. [PubMed: 20666414]
19. Shvartsburg AA, Smith RD. Anal Chem. 2011; 83:9159–9166. [PubMed: 22074292]
20. Shvartsburg AA, Smith RD. Anal Chem. 2011; 83:23–29. [PubMed: 21117630]
21. Shvartsburg AA, Mashkevich SV, Smith RD. J Phys Chem A. 2006; 110:2663–2673. [PubMed: 16494377]
22. Shvartsburg AA, Zheng Y, Smith RD, Kelleher NL. Anal Chem. 2012; 84:6317–6320. [PubMed: 22812477]
23. Shvartsburg AA, Singer D, Smith RD, Hoffmann R. Anal Chem. 2011; 83:5078–5085. [PubMed: 21667994]
24. Shvartsburg AA, Creese AJ, Smith RD, Cooper HJ. Anal Chem. 2011; 83:6918–6923. [PubMed: 21863819]
25. Purves RW, Barnett DA, Guevremont R. Int J Mass Spectrom. 2000; 197:163–177.
26. Purves RW, Barnett DA, Ells B, Guevremont R. J Am Soc Mass Spectrom. 2000; 11:738–745. [PubMed: 10937797]
27. Robinson EW, Williams ER. J Am Soc Mass Spectrom. 2005; 16:1427–1437. [PubMed: 16023362]
28. Shvartsburg AA, Bryskiewicz T, Purves RW, Tang K, Guevremont R, Smith RD. J Phys Chem B. 2006; 110:21966–21980. [PubMed: 17064166]
29. Shvartsburg AA, Li F, Tang K, Smith RD. Anal Chem. 2006; 78:3706–3714. [PubMed: 16737227]
30. Shvartsburg AA, Smith RD. J Am Soc Mass Spectrom. 2007; 18:1672–1681. [PubMed: 17723907]
31. Krylov EV, Nazarov EG, Miller RA. Int J Mass Spectrom. 2007; 266:76–85.

32. Counterman AE, Valentine SJ, Srebalus CA, Henderson SC, Hoaglund CS, Clemmer DE. J Am Soc Mass Spectrom. 1998; 9:743–759. [PubMed: 9692251]

33. Lee S, Ewing MA, Nachtigall FM, Kurulugama RT, Valentine SJ, Clemmer DE. J Phys Chem B. 2010; 114:12406– 12415. [PubMed: 20822127]

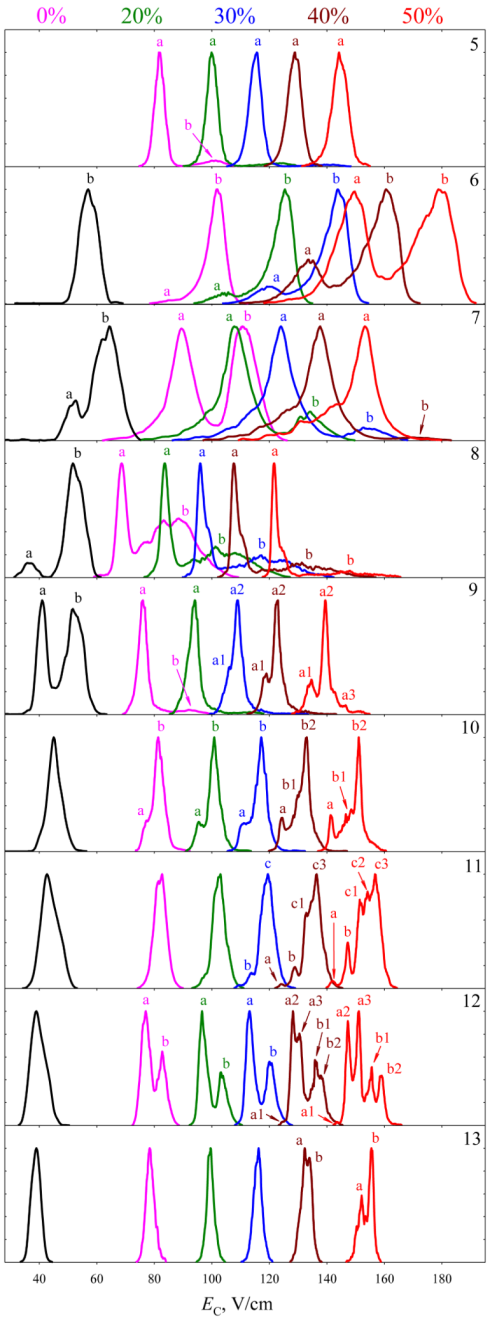

Fig. 1.

Normalized FAIMS spectra measured for ubiquitin ions with $z = 5 – 13$ (top to bottom, as marked) using E_D = 28 kV/cm and He/N_2 mixtures with 0 – 50% He (color-coded on the top). The benchmarks obtained using a cylindrical FAIMS analyzer with E_D = 20 kV/cm and N_2 in Ref. [7] are in black. Selected conformers are labeled to help following the structural transitions.

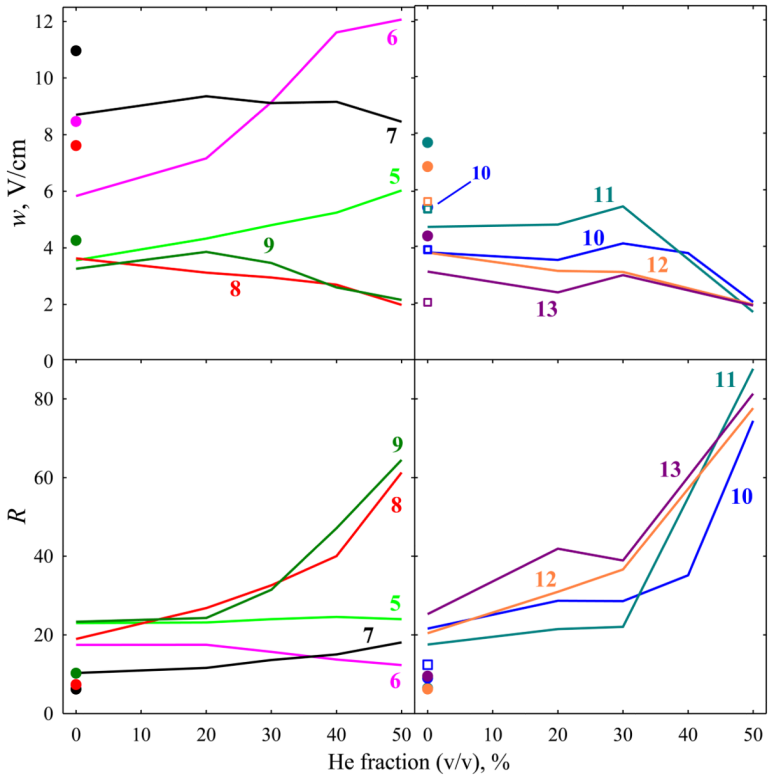

Fig. 2.

Peak widths and resolving power values for the major features in ubiquitin ion spectra with z = 5 – 9 (left column) and z = 10 – 13 (right column): lines and circles for the data in Fig. 1 with planar and cylindrical FAIMS devices, respectively; squares for the data obtained (for z = 10 – 13) using a planar analyzer with E_D = 20 kV/cm and N_2 in Ref. [29].

Table 1

Calculated and measured temperatures (°C) for ubiquitin ions in FAIMS

Conditions	Mean T_I (measured)[a]	For compact geometries[b]		For elongated geometries[b]	
		$<T_I>$	T_{max}	$<T_I>$	T_{max}
E_D = 20 kV/cm, N_2	70	34 – 38	78 – 93	30 – 33	58 – 74
E_D = 28 kV/cm, N_2	92	45 – 48	129 – 142	38 – 44	93 – 123
E_D = 28 kV/cm, He/N_2	125	54 – 58	167 – 185	43 – 52	118 – 159

[a]Weighted averages of T_I from matching DTIMS data for all charge states with multiple peaks.

[b]The temperatures in N_2 calculated assuming the mobilities measured (Ref. [15]) at peak apexes for z = 6 – 10, that is K_0 = 1.02 – 1.18 cm^2/(Vs) for "compact" families and 0.83 – 0.99 cm^2/(Vs) for elongated ones. The mobilities in 1:1 He/N_2 were estimated from the values in N_2 and He via the Blanc's law (Ref. [18]).